



# An endohedral fullerene-based nuclear spin quantum computer

Chenyong Ju<sup>a</sup>, Dieter Suter<sup>b</sup>, Jiangfeng Du<sup>a,\*</sup>

<sup>a</sup> Hefei National Laboratory for Physical Sciences at Microscale and Department of Modern Physics, University of Science and Technology of China, 230026 Hefei, People's Republic of China

<sup>b</sup> Fakultät Physik, Technische Universität Dortmund, D-44221 Dortmund, Germany

## ARTICLE INFO

### Article history:

Received 3 February 2011

Accepted 14 February 2011

Available online 18 February 2011

Communicated by P.R. Holland

### Keywords:

Quantum computation

Endohedral fullerene

Nuclear spin

## ABSTRACT

We propose a new scalable quantum computer architecture based on endohedral fullerene molecules. Qubits are encoded in the nuclear spins of the endohedral atoms, which possess even longer coherence times than the electron spins which are used as the qubits in previous proposals. To address the individual qubits, we use the hyperfine interaction, which distinguishes two modes (active and passive) of the nuclear spin. Two-qubit quantum gates are effectively implemented by employing the electronic dipolar interaction between adjacent molecules. The electron spins also assist in the qubit initialization and readout. Our architecture should be significantly easier to implement than earlier proposals for spin-based quantum computers, such as the concept of Kane [B.E. Kane, Nature 393 (1998) 133].

© 2011 Elsevier B.V. All rights reserved.

## 1. Introduction

Solid-state quantum computation is thought to hold the promise of building a large-scale quantum computer, which would be qualitatively more powerful than conventional computers for some specific problems [1–3]. Among the designs using solid-state materials, Kane's proposal [4], which uses donor nuclear spins in silicon, appears very attractive if the technical challenges can be overcome. Specifically, it requires donor atoms placed with nanometer precision inside a silicon crystal, which is rather difficult with today's technology.

This difficulty is avoided in the proposals based on endohedral fullerenes [5–9], in which the qubits are placed on the surface rather than inside the crystal. The C<sub>60</sub> molecule can serve as a handle for the arrangement of the qubits on the surface, which is possible with state of the art scanning tunneling microscopy (STM) techniques [10,11]. Its highly symmetric structure also provides a sheltering environment for the enclosed spin. The nitrogen and phosphorus atoms inside these cages are virtually free atoms, with very long relaxation times [5,7]. These properties make the endohedral fullerenes very promising for storing quantum information.

While the previous endohedral fullerene proposals mainly use the electron spins as qubits, here we propose a scalable quantum computer scheme based on the nuclear spins. The main advantage of using the nuclear spins is their even longer spin coherence

times, compared to the electron spins. The electron spins are used here as auxiliaries which help for addressing individual nuclear spin qubits, providing effective couplings between them, as well as for initialization and readout of the nuclear spin qubits. In this respect, our approach is similar to that of Kane, but it may incur fewer technical challenges.

## 2. Qubit implementation

We consider a chain of endohedral fullerene molecules (<sup>15</sup>N@C<sub>60</sub> or <sup>31</sup>P@C<sub>60</sub>) placed in an external magnetic field oriented along the z-direction. Each molecule contains a nuclear spin  $I = \frac{1}{2}$  and an electron spin  $S = \frac{3}{2}$ , whose Hamiltonian is in first order given by ( $\hbar = 1$ )

$$H_0 = g\mu_B B_0 S_z - \gamma_n B_0 I_z + A S_z I_z, \quad (1)$$

where the first two terms are the electron and nuclear Zeeman interactions and the last term is the hyperfine interaction.  $g$  is the electron g-factor,  $\mu_B$  is the Bohr magneton and  $\gamma_n$  the gyromagnetic ratio of the nucleus. In an external field of  $B_0 = 1$  T, the electron Larmor frequency is  $\nu_e \approx 28$  GHz and the nuclear Larmor frequency is  $\nu_n \approx 3.1$  MHz for <sup>15</sup>N and  $\nu_n \approx 17.3$  MHz for <sup>31</sup>P, while the hyperfine interaction is 21.2 MHz for <sup>15</sup>N and 138.4 MHz for <sup>31</sup>P [7]. Fig. 1 shows the related energy level diagram with the arrows indicating the magnetic-dipole allowed transitions. The hyperfine interaction splits the ESR spectrum into two lines (Fig. 2), each corresponding to three degenerate ESR transitions. The NMR spectrum consists of four nuclear spin transitions, corresponding to the four electron spin states [12]. Both spins can be manipulated by resonant radio-frequency (rf) and microwave pulses respectively.

\* Corresponding author at: Department of Modern Physics, University of Science and Technology of China, 230026 Hefei, China. Tel.: +86 551 3600307; fax: +86 551 3600039.

E-mail address: djf@ustc.edu.cn (J. Du).

The Hamiltonian of the linear chain of  $N$  endohedral fullerenes (with the same molecules) is

$$H_{\text{chain}} = \sum_{i=1}^N (\Omega_S^i S_z^i - \Omega_I^i I_z^i + A S_z^i I_z^i) + \sum_{i < j} D_{ij} S_z^i S_z^j, \quad (2)$$

where the first term is the Hamiltonian for each molecule, and the second term contains the truncated dipolar interactions between the electron spins.  $\Omega_S^i = g\mu_B B^i$  is the Larmor frequency of the  $i$ th electron spin, which experiences the field  $B^i = B_0 + B_G^i$ , where  $B_G^i$  describes the position-dependent component used to address the electron spins. Similarly,  $\Omega_I^i = \gamma_n B^i$  is the nuclear Larmor frequency of the same molecule. The magnetic dipole–dipole coupling between the electron spins is the only strong coupling between the molecules [13], with the coupling strength  $D_{ij} \propto (1 - 3 \cos^2 \theta) / r_{ij}^3$ , where  $r_{ij} = |\vec{r}_{ij}|$  is the distance between the electron spins and  $\theta$  is the angle between  $\vec{r}_{ij}$  and  $\vec{B}$ . To have specific numbers, we will in the following assume that  $r = 3.5$  nm is the spacing between nearest neighbors and  $\theta = 90^\circ$ . This corresponds to a coupling strength of  $D_{ij} = D_0 / (j - i)^3$  between the  $j$ th and  $i$ th electron spins, with  $D_0 \approx 0.92$  MHz. As discussed below, under the conditions assumed here, the corresponding frequency difference between the  $j$ th and  $i$ th electron spins is  $\approx 39(j - i)$  MHz  $\gg D_{ij}$ . The truncation of the dipole–dipole coupling is therefore very well justified.

Qubits are encoded in the nuclear spins. To address a specific qubit, we need a way to distinguish between them. In Kane's proposal [4], electrodes that access individual molecules (the  $A$ -gates) are used to control the resonance frequencies of the donor  $^{31}\text{P}$  nuclear spins. However, this method still remains technically very challenging and has not been implemented so far. Magnetic field gradients were proposed as an alternative addressing mechanism [6]. If currents of  $I = 1$  A flow through 2 parallel wires at

a distance of 1  $\mu\text{m}$ , they generate a magnetic field gradient of  $\approx 4$  G/nm. This yields a frequency difference between the electron spins of adjacent molecules (which are 3.5 nm apart) of  $\approx 39$  MHz.

The corresponding frequency differences for adjacent nuclear spins are much smaller: 4.3 kHz for  $^{15}\text{N}$  and 24.2 kHz for  $^{31}\text{P}$ . Applying selective pulses at such small frequency differences would result in very slow gate operations lasting several hundred microseconds.

Here we propose a method to effectively address the nuclear spins with the assistance of the electron spins. Due to the electron–nuclear hyperfine interaction (Eq. (1)), the different electron spin states would yield different local magnetic fields on its corresponding nuclear spin, resulting in different transition frequencies. For example, the frequencies of the  $^{15}\text{N}$  nuclear spin corresponding to the two electron spin states  $|-\frac{3}{2}\rangle$  and  $|\frac{3}{2}\rangle$  differ by  $\approx 2\nu_n \approx 6.2$  MHz when  $B_0 = 1$  T. For  $^{31}\text{P}$  it is even larger. In our scheme we utilize this effect to achieve the nuclear spin addressing. Specifically, we distinguish two modes of an individual nuclear spin: the *passive mode*, which corresponds to the electron spin state  $|-\frac{3}{2}\rangle$  and the *active mode*, which corresponds to the electron spin state  $|\frac{3}{2}\rangle$ . These two modes of the nuclear spin have very distinct resonance frequencies (see Fig. 2) and we can switch between them by flipping the electron spin with selective microwave  $\pi$  pulses. When the quantum computer is idle all the electron spins stay in its ground state  $|-\frac{3}{2}\rangle$ , and hence all the nuclear spins are in their passive modes. If one needs to operate on a specific nuclear spin, it is first switched to the active mode by flipping its corresponding electron spin to the state  $|\frac{3}{2}\rangle$ . The nuclear spin in the active state can be individually manipulated by resonant rf pulses (with a speed  $\sim 1$   $\mu\text{s}$ ), without affecting the passive qubits. Afterwards the nuclear spin is switched back to its passive mode by flipping the corresponding electron spin back to the state  $|-\frac{3}{2}\rangle$ . The above procedure achieves the addressing of the nuclear spins.

The nuclear spin addressing method presented here requires no additional apparatus as long as the electron spins are addressed. As mentioned above the latter may be realized by the magnetic field gradients method with existing technology. The requirement that the electron spins are fully polarized to its ground state is a natural consequence of the initialization step of the quantum computer and can be achieved within reasonable experimental conditions, as discussed below. This initialization ability is a basic requirement for all physical implementations of quantum computation [14]. Besides, since the electron spin states  $|-\frac{3}{2}\rangle$  and  $|\frac{3}{2}\rangle$  are the eigenstates of the static Hamiltonian (Eq. (2)), and the electron spins in fullerenes possess a very long spin–lattice relaxation time ( $\geq 1$  s at a temperature of 5 K [5] and much larger in the mK region), the two electron spin states can be well preserved during the computation.

The magnetic field gradient used for addressing the electron spins also results in a frequency distribution of the nuclear spins.

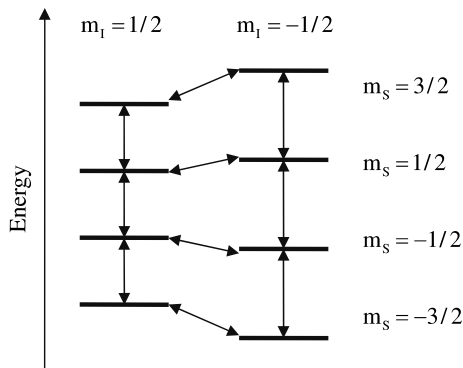


Fig. 1. The energy level diagram of endohedral fullerene ( $^{15}\text{N}@C_{60}$  or  $^{31}\text{P}@C_{60}$ ). The vertical arrows indicate the allowed electronic transitions ( $\Delta m_s = \pm 1$ ) and horizontal arrows indicate the allowed nuclear transitions ( $\Delta m_I = \pm 1$ ).

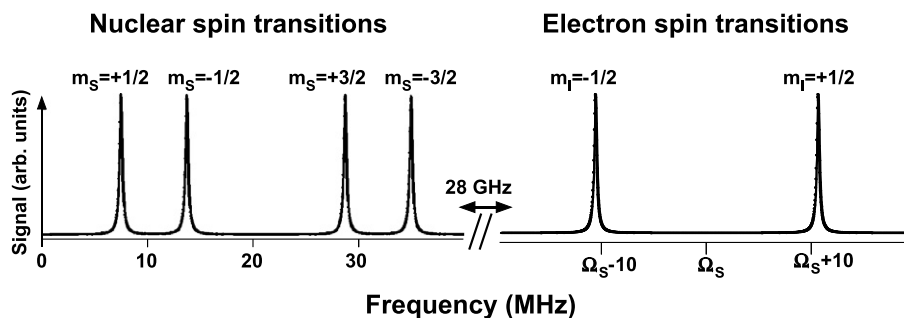


Fig. 2. Allowed magnetic resonance transitions of  $^{15}\text{N}@C_{60}$  ( $B_0 = 1$  T). The transition frequencies of the nuclear spin (low-frequency range) are labeled with the corresponding states of the electron spin and vice versa. The amplitudes of the electron- and nuclear transitions correspond to the high-temperature limit and the nuclear spin transitions are in reality much weaker than the electron spin transitions.

This limits the number of spins addressable in the present scheme. If we want to ensure that the frequency difference between an active nuclear spin and the passive nuclear spins is  $> \nu_{\min} = 2$  MHz, we find for the maximum number of qubits is  $N_{\max} \leq (2\nu_n - \nu_{\min})/\Delta\nu$ , where  $\Delta\nu$  is the frequency difference between adjacent nuclear spins. For the parameters given above, we find  $N_{\max} \approx 1000$  for  $^{15}\text{N}$  and  $N_{\max} \approx 1300$  for  $^{31}\text{P}$ . This number can be further enhanced by increasing the external magnetic field.

The possible overlaps of the electronic hyperfine lines in the array should also be considered. However, this always can be avoided by an appropriate choice of the parameters. Suppose the frequency difference between neighboring electron spins caused by magnetic field gradient is  $\Delta$ , and the hyperfine coupling strength is  $a$ , then the minimum separation of the electronic hyperfine lines in the array is  $\min\{|(j-i)\Delta - a|, \Delta\}$ . For the parameters chosen in our model, this value is 17.8 MHz for  $^{15}\text{N}$  and 17.6 MHz for  $^{31}\text{P}$ : in this case, overlap does not occur.

### 3. Quantum gates

Universal quantum computation requires the ability to perform arbitrary gate operations. General gate operations can be decomposed into one-qubit rotations with arbitrary angles and one suitable two-qubit gate, such as the controlled-NOT gate. As for any spin-qubit, one-qubit gates can be implemented by resonant rf pulses that rotate the corresponding nuclear spin, which must be in the *active* state. Two-qubit gates cannot be implemented directly, since there is no significant interaction between the nuclear spins. Here, we again use the assistance of the electron spins, which interact via magnetic dipole–dipole couplings. In Ref. [15] we proposed a scheme to realize two-qubit gates on nuclear spins in the heteronuclear system of two neighboring  $^{15}\text{N}@C_{60}$  and  $^{31}\text{P}@C_{60}$  molecules. Here, combined with the above qubit-addressing method, we generate the gate scheme to the homonuclear case, which is applicable to the scalable linear chain.

Our two-qubit gate operation between adjacent nuclear spin qubits uses two electronic and two nuclear spins, which we denote as  $S_1$  and  $S_2$  and  $I_1$  and  $I_2$ , respectively. The full operation can be decomposed into three steps: (i) Transfer the information from the nuclear spin  $I_1$  through the electron spin  $S_1$  to the electron spin  $S_2$ . (ii) Apply the target two-qubit operation to the spins  $S_2$  and  $I_2$ . (iii) Transfer the information from  $S_2$  back to  $I_1$ . The first step, corresponding to the transfer  $I_1 \rightarrow S_2$  can be implemented by the two operations

$$U_{S_1 I_1}: [-S_{1y}^{1/2} I_{1x}] - [-I_{1x}^{3/2} S_{1y}], \quad (3)$$

$$U_{S_2 S_1}: [S_{2x}^{3/2} S_{1y}] - [S_{1y}^{3/2} S_{2x}]. \quad (4)$$

Here the notation  $[A] = e^{-i\pi A}$  is used. The term  $[-S_{1y}^{1/2} I_{1x}]$  represents a rotation of the spin  $S_1$  around the  $-y$  axis by an angle  $\pi$ , conditional on the coupled nuclear spin being in the state  $|\frac{1}{2}\rangle$ . Similarly,  $[-I_{1x}^{3/2} S_{1y}]$  represents a  $(\pi)_x$  rotation of the nuclear spin if the electron spin state is  $|\frac{3}{2}\rangle$ , and  $[S_{2x}^{3/2} S_{1y}]$  represents a selective microwave  $(\pi)_x$  pulse on the second electron spin ( $S_2$ ) conditional on the first electron spin ( $S_1$ ) being in the state  $|\frac{3}{2}\rangle$ . The above pulse sequence uses the fact that the initial states of all electron spins are  $|\frac{3}{2}\rangle$ . The  $U_{S_1 I_1}$  operation transforms the nuclear-electron spin state  $(\alpha, \beta)^T \otimes (0, 0, 0, 1)^T$  into  $(0, 1)^T \otimes (i\alpha, 0, 0, \beta)^T$  and the  $U_{S_2 S_1}$  operation transforms the two-electron spin state  $(i\alpha, 0, 0, \beta)^T \otimes (0, 0, 0, 1)^T$  into  $(0, 0, 0, 1)^T \otimes (-\alpha, 0, 0, \beta)^T$ .

Note that after the first pulse in  $U_{S_1 I_1}$  the nuclear spin is entangled with the electron spin, resulting in the state  $\alpha|\frac{1}{2}\rangle|\frac{3}{2}\rangle_S +$

$\beta|-\frac{1}{2}\rangle|-\frac{3}{2}\rangle_S$ . The nuclear spin is partly in the active mode (the subspace corresponding to the electron spin state  $|\frac{3}{2}\rangle_S$ ) and partly in the passive mode (the  $|-\frac{3}{2}\rangle_S$  subspace). Since the second pulse in  $U_{S_1 I_1}$  affects only the active mode subspace, this operation does not conflict with the nuclear spin addressing scheme and does not influence the states of the passive nuclear spins.

The next step is to perform a CNOT gate between  $S_2$  and  $I_2$  by a selective rf pulse  $[-I_{2x}^{3/2} S_{2y}]$ , which acts on  $I_2$ 's active mode subspace. Finally, the information encoded on  $S_2$  is transferred back to  $I_1$  by  $U_{S_1 S_2}^{-1}$  and  $U_{S_1 I_1}^{-1}$ . After this step, the overall propagator for the two nuclear spins is  $U_{\text{CNOT}} = 2i|\frac{1}{2}\rangle\langle\frac{1}{2}| \otimes I_{2x} + |-\frac{1}{2}\rangle\langle-\frac{1}{2}| \otimes I_2$ , where  $I_2$  is the identity operator on  $I_2$ . All the electron spins are returned to the initial state  $|\frac{3}{2}\rangle$ . If necessary, the phase factor  $i$  can be eliminated by a phase gate  $e^{-i\frac{\pi}{2} I_{1z}}$  performed on  $I_1$ . This results in a standard CNOT gate  $2|\frac{1}{2}\rangle\langle\frac{1}{2}| \otimes I_{2x} + |-\frac{1}{2}\rangle\langle-\frac{1}{2}| \otimes I_2$ , up to an irrelevant overall phase factor.

Other nontrivial two-qubit gates, like the controlled-rotation gate and the controlled-phase gate, can be implemented in a similar way by changing the  $S_2$  controlled NOT gate into a controlled rotation or phase gate. In those cases, a different phase gate may be required in the final step.

There is another way to implement the CNOT gate: first we transfer the information encoded on  $I_1$  and  $I_2$  to  $S_1$  and  $S_2$  by the operations  $U_{S_1 I_1}$  and  $U_{S_2 I_2}$  respectively. Then we can realize a CNOT gate between the two electron spins by the selective microwave pulse  $[S_{2x}^{3/2} S_{1y}]$  applied to  $S_2$ . Finally, the information encoded on  $S_1$  and  $S_2$  is transferred back to  $I_1$  and  $I_2$  by  $U_{S_1 I_1}^{-1}$  and  $U_{S_2 I_2}^{-1}$  respectively. If required, the additional phases can then be corrected. This implementation provides some advantage in speed, since the operations  $U_{S_1 I_1}$  and  $U_{S_2 I_2}$  (and hence  $U_{S_1 I_1}^{-1}$  and  $U_{S_2 I_2}^{-1}$ ) can be carried out in parallel, i.e., the two  $[-I_x^{3/2} S_y]$  operations for  $I_1$  and  $I_2$  can be realized simultaneously.

The above analysis is somewhat simplified in that it only includes the effect of couplings between the spins that are directly involved in the operations. In addition, we have to include the effect of couplings to passive spins. In the case of the electron spins, this is relatively straightforward: since all passive electron spins are in the state  $|\frac{3}{2}\rangle$ , each qubit  $j$  only shifts the frequency at which the selective pulses have to be applied by  $-3D_{ij}/2$  [16]. During the  $U_{S_1 S_2}$  operation, the nuclear spins split the resonance lines of the electron spins in the same molecule into two. Since the pulses applied to the electron spins must be selective, they cannot be strong compared to the hyperfine coupling. However, we can apply bichromatic pulses that drive the transitions associated with the two nuclear spin states simultaneously. This eliminates the effect of the hyperfine coupling on the operations within the Hilbert space of the electron spins.

All the pulses used in the present quantum gate scheme can be implemented with existing magnetic resonance technology, as demonstrated in Refs. [12,17]. A rough estimation of the gating times is about 1  $\mu\text{s}$  for one-qubit gates and 6  $\mu\text{s}$  for two-qubit gates, using the numbers considered above. Therefore within the spin coherence time ( $\geq 1$  s in a careful design [7]) at least  $10^5$ – $10^6$  quantum gates can be performed.

An important advantage of this scheme is that it does not require the control of the inter-qubit couplings, switching the couplings on and off during the computation. There is no significant coupling between the nuclear spin qubits, and the always-on electron dipolar interaction does not affect the nuclear spins, but it provides the necessary coupling for implementing the two-qubit gates. This advantage reduces the technical challenges compared to other nuclear spin-based quantum computer architectures, such as Kane's proposal.

#### 4. Qubit initialization

To allow quantum computation, the spins must be initialized into a well-defined state before starting a quantum computation [14]. Usually, this can be achieved by cooling the system to low temperatures so that the spins are in their ground states. Polarizing the electron spins is far easier than the nuclear spins. At a temperature of 100 mK, in an external field of  $B_0 = 2$  T, the electron spins are almost completely polarized, with  $n_{\uparrow}/n_{\downarrow} < 10^{-6}$ . This thermal initialization cannot be applied to the nuclear spins, but we can transform the electron spin polarization to the nuclear spins by the  $U_{SI}$  operation of Eq. (3), and thus completely polarize the nuclear spins. Afterwards the electron spins are polarized again under the above conditions. The fact that the spin-lattice relaxation time of the nuclear spins (several hours for  $^{15}\text{N}@C_{60}$  molecules at 4.2 K [18]) is far longer than that of electron spins guarantees the feasibility of this initialization procedure. The  $U_{SI}$  operation can be applied in parallel for all molecules by turning off the magnetic field gradients during the initialization procedure.

A much bigger challenge is the requirement to continuously supply fresh qubits in a well defined state during the computation, which is needed for quantum error correction. In the present architecture, the individual nuclear spins can be refreshed by exchanging their state with that of the electron spin, whose state is known and stays in its ground state for the most time. This is accomplished again by the  $U_{SI}$  operation. Refreshing an individual electron spin may be achieved by the projective single-spin measurement discussed below.

#### 5. Readout

The measurement of the nuclear spin (the qubit) is achieved by first transforming its state to the electron spin using the  $U_{SI}$  operation and then measuring the electron spin. Measuring the state of single electron spins remains a challenge, particularly if they are well isolated, as in  $\text{N}@C_{60}$  [8,9,19], but it has been demonstrated for this particular system on the basis of tunneling spectroscopy [20].

#### 6. Conclusion

A scalable quantum computer scheme is proposed based on endohedral fullerene molecules. The qubits are encoded in the nu-

clear spins of the encapsulated atoms and the electron spins assist in the addressing, two-qubit quantum gates, initialization, and detection of the nuclear spin qubits. Compared to previous nuclear spin-based scalable quantum computer schemes such as Kane's proposal, the present scheme should be easier to implement. The required apparatus has to generate magnetic field gradients by micron-sized wires, while electrodes patterned on the nm scale (the A-gates) are used in Kane's proposal. Furthermore, the present proposal does not require switching on and off the inter-qubit coupling and the qubits are placed on the surface rather than inside the silicon as in Kane's proposal.

#### Acknowledgements

This work was supported by the Key Program of NNSFC (Grant No. 10834005), the CAS, and the NFRP (Grant No. 2007CB925200).

#### References

- [1] D. Deutsch, R. Jozsa, Proc. R. Soc. London A 439 (1992) 553.
- [2] P.W. Shor, SIAM J. Sci. Stat. Comput. 26 (1997) 1484.
- [3] L.K. Grover, Phys. Rev. Lett. 79 (1997) 325.
- [4] B.E. Kane, Nature 393 (1998) 133.
- [5] W. Harneit, Phys. Rev. A 65 (2002) 032322.
- [6] D. Suter, K. Lim, Phys. Rev. A 65 (2002) 052309.
- [7] J. Twamley, Phys. Rev. A 67 (2003) 052318.
- [8] S.C. Benjamin, et al., J. Phys.: Condens. Matter 18 (2006) s867.
- [9] W. Harneit, K. Huebener, B. Naydenov, S. Schaefer, M. Scheloske, Phys. Status Solidi B 244 (2007) 3879.
- [10] P. Moriarty, Y.R. Ma, M.D. Upward, P.H. Beton, Surf. Sci. 407 (1998) 27.
- [11] M.J. Butcher, et al., Appl. Phys. Lett. 75 (1999) 1074.
- [12] M. Mehring, W. Scherer, A. Weidinger, Phys. Rev. Lett. 93 (2004) 206603; W. Scherer, M. Mehring, J. Chem. Phys. 128 (2008) 052305.
- [13] The interaction between the neighboring nuclear spins is of the order of a few hertz, and the dipolar hyperfine coupling between the electron spin and the neighboring nuclear spin is of the order of 7 kHz, all at a separation of 1 nm. On the time scales relevant to us, these interactions can be safely neglected.
- [14] D.P. DiVincenzo, Fortschr. Phys. 48 (2000) 771.
- [15] C. Ju, D. Suter, J. Du, Phys. Rev. A 75 (2007) 012318.
- [16] W.L. Yang, Z.Y. Xu, H. Wei, M. Feng, D. Suter, Phys. Rev. A 81 (2010) 032303.
- [17] J.J.L. Morton, et al., Nat. Phys. 2 (2006) 40.
- [18] G.W. Morley, et al., Phys. Rev. Lett. 98 (2007) 220501.
- [19] M. Feng, J. Twamley, Phys. Rev. A 70 (2004) 030303(R).
- [20] J.E. Grose, et al., Nat. Mater. 7 (2008) 884.